



HAL
open science

Sharp optical phonon softening close to optimal doping in $\text{La}_{2-x}\text{Ba}_x\text{CuO}_{4+\delta}$

Matteo d'Astuto, Guy Dhalenne, Jeff Graf, Moritz Hoesch, Paola Giura,
Michael Krisch, Patrick Berthet, Alessandra Lanzara, Abhay Shukla

► **To cite this version:**

Matteo d'Astuto, Guy Dhalenne, Jeff Graf, Moritz Hoesch, Paola Giura, et al.. Sharp optical phonon softening close to optimal doping in $\text{La}_{2-x}\text{Ba}_x\text{CuO}_{4+\delta}$. *Physical Review B: Condensed Matter and Materials Physics* (1998-2015), 2008, 78, pp.140511(R). 10.1103/PhysRevB.78.140511 . hal-00311976v3

HAL Id: hal-00311976

<https://hal.science/hal-00311976v3>

Submitted on 1 Oct 2008

HAL is a multi-disciplinary open access archive for the deposit and dissemination of scientific research documents, whether they are published or not. The documents may come from teaching and research institutions in France or abroad, or from public or private research centers.

L'archive ouverte pluridisciplinaire **HAL**, est destinée au dépôt et à la diffusion de documents scientifiques de niveau recherche, publiés ou non, émanant des établissements d'enseignement et de recherche français ou étrangers, des laboratoires publics ou privés.

Sharp optical phonon softening close to optimal doping in $\text{La}_{2-x}\text{Ba}_x\text{CuO}_{4+\delta}$

Matteo d'Astuto,^{1,*} Guy Dhalenne,² Jeff Graf,³ Moritz Hoesch,⁴ Paola Giura,¹

Michael Krisch,⁴ Patrick Berthet,² Alessandra Lanzara,^{3,5} and Abhay Shukla¹

¹*Institut de Minéralogie et de Physique des Milieux Condensés (IMPMC),*

Université Pierre et Marie Curie - Paris 6, case 115, 4, place Jussieu, 75252 Paris cedex 05, France[†]

²*Laboratoire de Physico-Chimie de l'Etat Solide (ICMMO), CNRS UMR8182,*

Université Paris-Sud 11, Bâtiment 410, 91405 Orsay, France

³*Materials Sciences Division, Lawrence Berkeley National Laboratory, Berkeley, CA 94720, USA*

⁴*European Synchrotron Radiation Facility, BP 220, F-38043 Grenoble Cedex, France*

⁵*Department of Physics, University of California Berkeley, CA 94720, USA*

(Dated: October 1, 2008)

We report a direct observation of a sharp Kohn-like anomaly in the doubly degenerate copper-oxygen bond-stretching phonon mode occurring at $\mathbf{q} = (0.3, 0, 0)$ in $\text{La}_{2-x}\text{Ba}_x\text{CuO}_{4+\delta}$ with $x = 0.14 \pm 0.01$, thanks to the high \mathbf{Q} resolution of inelastic x-ray scattering. This anomaly is clearly seen when the inelastic signal is analysed using a single mode but is also consistent with a two mode hypothesis possibly due to a splitting of the degenerate modes due to symmetry breaking stripes. Our observation shows that the effect persists at the stripe propagation vector in a superconducting system close to optimal doping.

I. INTRODUCTION

Copper-oxygen bond stretching modes in high-temperature superconducting cuprate (HTCS) have long been known to show anomalies related to doping¹. The origin of the anomalies is still an open issue. Along with electron-phonon coupling effects, a mechanism involving the formation of an inhomogeneous charge state, also known as *stripes*^{2,3,4,5,6} has been discussed^{7,8}. At the outset let us clarify the anomalies seen in this phonon mode. Earlier works¹ focused on the gradual softening of this mode with doping, a phenomenon seen quite universally in HTCS and now relatively well understood, even theoretically⁹ on the basis of electron-phonon coupling and screening mechanisms which come into play on doping. This softening can be well described by a cosine-like behaviour of the mode with its minimum at the zone boundary. Even in the earliest works, however, there were indications that the dispersion might be more complicated, with deviations from the cosine-like shape⁷. The possibility that these deviations are caused by stripes has been invoked and adopted in a recent paper¹⁰ in which previous data on HTCS, are compared to newer ones, in particular for $\text{La}_{2-x}\text{Ba}_x\text{CuO}_{4+\delta}$ with $x=1/8$. In this system, for $x \sim 1/8$, an anomalous suppression of the superconductivity reported in Ref. 11 was later shown to be associated with charge and spin stripe order^{12,13,14}. Signatures of stripes in superconducting samples remain elusive, though it was proposed that stripes are difficult to detect in these because they are no longer static^{15,16}. Using phonons to probe charge fluctuations can potentially lead to a reliable signature of static and dynamic stripes in HTCS. The authors of Ref. 10 in describing their high resolution inelastic neutron scattering data of the copper-oxygen bond stretching mode, show how one of its two normally degenerate components follows the expected cosine-like dispersion while the other deviates presenting a much sharper dip. They interpret this behaviour as a Kohn-like anomaly due to stripes which lift the degeneracy.³² This scenario is very intriguing, nevertheless, the dip is not directly visible in the data of Ref. 10, and the authors deduce its existence from a broad shoulder on the low energy side of the Cu-O bond stretching phonon mode. Thus, as we show in a recent paper¹⁷, it is desirable to have a direct measurement of the dip since without it, other reasons could be invoked to explain the observed signal. To clarify this point we have carried out a high (\mathbf{Q}, ω) -resolution measurement in $\text{La}_{2-x}\text{Ba}_x\text{CuO}_{4+\delta}$ using Inelastic X-ray Scattering (IXS), with a comparable energy resolution, but with a higher resolution in reciprocal space compared to previous inelastic neutron scattering experiments.

This allowed us not only to confirm the presence of a dip around $\mathbf{q} = (0.3, 0, 0)$ in the dispersion of the copper-oxygen bond stretching mode, but also to extend this observation to superconducting doping value ($x = 0.14$). This doping level leads to a stripe-propagation-vector $\mathbf{q} \approx (0.3, 0, 0)$ ⁶, in striking agreement with our findings, and supports a picture based on the interaction with stripes^{7,10}.

*matteo.dastuto@imPMC.jussieu.fr

[†]Institut de Minéralogie et de Physique des Milieux Condensés (IMPMC), CNRS UMR 7590, Campus Boucaut, 140 rue de Lourmel, 75015 Paris, France

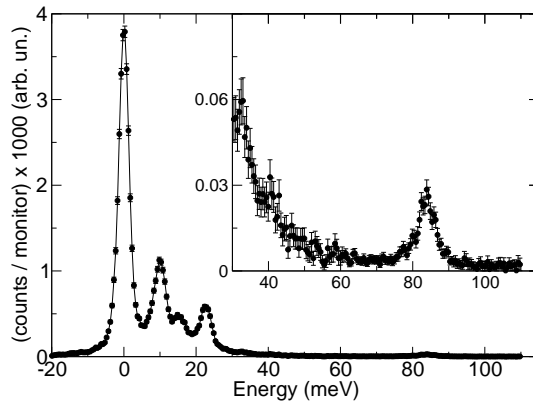


FIG. 1: Inelastic x-ray scattering example spectrum of $\text{La}_{1.86}\text{Ba}_{0.14}\text{CuO}_{4+\delta}$, at $\mathbf{Q} = (3.11, 0.04, 0)$. At zero energy one observes the elastic line, while at positive energy, several phonon modes are observed corresponding to Stokes processes. In the inset we zoom on to the high energy optical Cu-O bond stretching mode. Anti-Stokes modes are not visible because of the unfavorable detailed balance at low temperature.

II. EXPERIMENT

We studied a single crystal of $\text{La}_{2-x}\text{Ba}_x\text{CuO}_{4+\delta}$ grown from the melt in an image furnace by the traveling solvent zone method, under a pressure of 3 bar oxygen. The measured $T_c = 18.1$ K with $\Delta T_c = 7$ K defined as the temperature range from 90% to 10% of the maximum Meissner signal, is consistent with micro-probe results indicating a content of $x = 0.14 \pm 0.01$ ¹⁸. The experiment was carried out at the IXS beamline II (ID28) at the European Synchrotron Radiation Facility in Grenoble. The sample was mounted in reflection geometry, on the cold finger of a closed-loop helium cryostat, in order to keep it at constant temperature $T = (17.8 \pm 0.5)$ K during the experiment. The low temperature was chosen so as to optimize the signal of the high energy modes over the tails of low energy ones. The sample c crystal axis was perpendicular to the scattering plane. We consider the tetragonal unit cell with $\alpha = \beta = \gamma = 90^\circ$ and the axes a and b along the Cu-O bond. The sample was aligned along $(H, 0, 0)$, and we refined the parameter $a = 3.792 \pm 0.001$ Å, according to the $\theta - 2\theta$ scan on the $(4, 0, 0)$ reflection, and adopted the value of $c = 13.235$ Å. The rocking curve at the $(4, 0, 0)$ reflection had a FWHM $\sim 0.06^\circ$, indicating a very low mosaic spread in the small volume probed. The IXS multi-analyzer spectrometer^{19,20} configurations chosen were of type $\mathbf{Q} = \mathbf{G} + \mathbf{q} = (3, 0, 0) + (q_x, q_y, 0)$, with simultaneous measurements from 7 analyzers. We collected data from the first 5 analyzers closer to the beam direction, which are at fixed angular spacing of $\sim 0.75^\circ$ ($q_x \sim \pm 0.07$), with the third one in longitudinal condition $q_y = 0$ while for the others $q_y \leq \pm 0.045$. This setup corresponds to the 3rd extended Brillouin Zone, where the zone center Γ is at $(4, 0, 0)$ and the extended zone boundary at $(3, 0, 0)$. The standard or folded zone boundary is at the point $M = (3.5, 0, 0)$. The scattering vector resolution was set using a slit opening in front of the analyzers of $h \times v = 20 \times 60$ mm corresponding to a solid angle of $\delta\theta \times \delta\xi = 0.19^\circ \times 0.57^\circ$. The resolution in the reciprocal space for 0.6968 Å wave-length was $(\pm\delta q_x, 0, 0)$ with $\delta q_x \approx 0.009$. The high energy resolution is obtained using the back-scattering silicon monochromator aligned along the $(1\ 1\ 1)$ direction^{21,22}. In the present experiment we choose to work with the Si $(9\ 9\ 9)$ reflection order, with a wave-length of 0.6968 Å (17794 eV) and an energy resolution $\Delta E = 3.0 \pm 0.2$ meV. An example of a raw IXS spectrum is given in Fig. 1. The energy scans were fitted using a sum of pseudo-Voigt for elastic and resolution-limited inelastic contributions, with parameters fixed to match the instrumental function, while a Lorentzian line-shape was used to fit modes with an intrinsic width larger than the instrumental resolution. In order to assign the measured phonon modes, we performed a lattice dynamical calculation using a computer code²³ based on a shell model²⁴. More details on analysis and simulation are described elsewhere¹⁷.

III. RESULTS AND DISCUSSION

The high energy portion of some typical measurements is shown in Fig. 2. In this spectral window, at least two modes could be identified: a mode at about 60 meV, corresponding to the 5th longitudinal optic mode (in order from the lowest energy), and a second dispersing from about 90 meV down to about 70 meV, the highest (6th) energy longitudinal Cu-O bond-stretching (or half breathing) optic mode. The fast downward dispersion is accompanied by a rapid broadening from 5 meV to about 15 meV FWHM. This mode is doubly degenerate, and could eventually

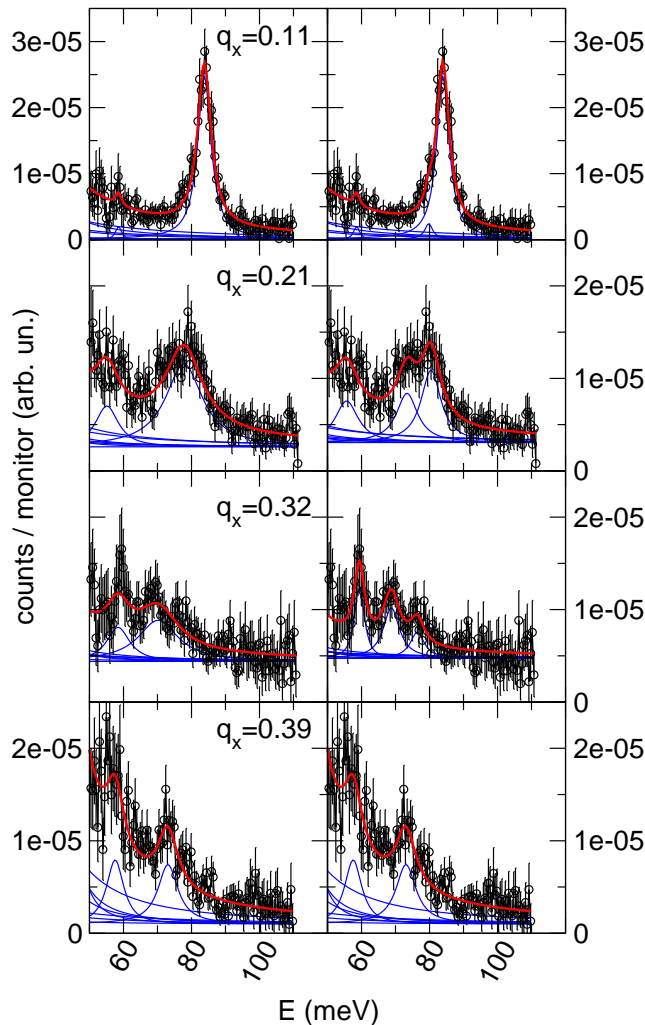


FIG. 2: (Color online) Inelastic X-ray scattering example spectra from $\text{La}_{1.86}\text{Ba}_{0.14}\text{CuO}_{4+\delta}$, at different wave-vectors $\mathbf{Q} = (3 + q_x, q_y, 0)$ (see text). In the left column the data are fitted using the degenerate Cu-O bond stretching mode hypothesis. In the right column the data are fitted supposing two Cu-O bond stretching mode.

split if the local symmetry is lowered by some anisotropy. Such splitting has been suggested¹⁰ for a $q_x \sim 0.2 - 0.3$, corresponding to the propagation vector of a charge modulation (“stripe”). Other possible origins of the double modes have been previously reported^{7,25} always in connection with microscopic phase-separation. The doubling of the modes can contribute to the observed broadening if the energy resolution is not enough to distinguish the two modes as in our case. In most of the measured spectra it is then not possible to have independent fitted parameters for frequency, intensity and width of each mode. We have used the error estimation of the fitted widths as a goodness of fit criterion and only in the case of $q_x = 0.32$ (see Fig. 2), the two mode fit appears to be better than the single mode fit for our data.

In Fig. 3 we show the results of our fitting for the frequencies (left panel) and width (right panel) for the single mode (blue circles). A minimum at $q_x = 0.32 \pm 0.04$ is clearly observed. In the same figure, we also show the results for the fit in a double mode hypothesis (red squares), for $q_x = 0.32$.

The difficulty of the analysis (the impossibility of reliably fitting two closely placed peaks) is inherent to the experimental strategy chosen: in order to follow in detail the dispersion we chose a higher \mathbf{Q} -resolution with comparable energy resolution to Ref. 10. This also results in a significantly different line-shape. In Ref. 10, using inelastic neutron scattering, the highest mode appears more intense because it is weakly dispersing, and thus benefits from a large \mathbf{Q} integration, while the low energy one appears broader because the supposed Kohn-like dip in the dispersion is only as large as the experimental \mathbf{Q} -resolution. Assuming that the two-mode hypothesis is valid let us examine the consequences for our data. A \mathbf{Q} -resolution narrower than the dip width results in a sharper low energy mode. We have already seen that the intensity of the high energy mode decreases due to the better \mathbf{Q} -resolution. This results

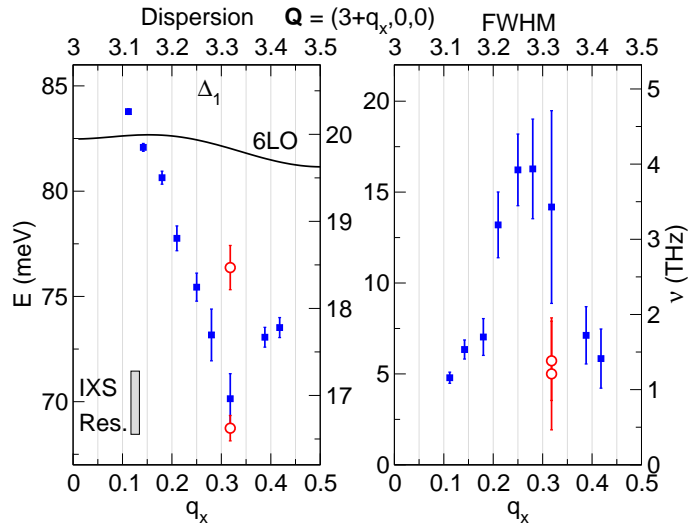


FIG. 3: (Color online) Left panel: $\text{La}_{1.86}\text{Ba}_{0.14}\text{CuO}_{4+\delta}$ Cu-O bond stretching (BS) dispersion. Blue square represent frequencies from the model fit with one mode, while red hollow circles represent a fit with two modes. The line correspond to a shell model lattice dynamics calculation. Right panel: $\text{La}_{1.86}\text{Ba}_{0.14}\text{CuO}_{4+\delta}$ Cu-O bond stretching (BS) width, symbols as above.

in two modes of similar intensity and width, more difficult to separate with this energy resolution. Returning to the results shown in Fig. 3, in a one mode hypothesis, we obtain a maximum of the width around $q_x \sim 0.3$, coinciding with the dispersion minimum. Indeed, even a one peak fit gives a well pronounced anomalous dip that is inconsistent with a cosine-like dispersion. The dip is observed even with a one peak fit because the dispersion of the concerned mode and its intensity are strong enough and dominate even after averaging with the less dispersing higher energy mode. The maximum in the width is, in fact, a measure of the energy distance between the modes which is associated with the dip, as already pointed out (see Fig. 4 in Ref. 10). Note that we extended the observation of this anomaly to a doping range which is well beyond the singular 1/8th level and crucially in a superconducting range where the stripes should be dynamic. Consistent with this higher doping level we observe that the dip is more spread out over the BZ, already starting at $q_x \approx 0.1$ with a FWHM of 4.7 ± 0.3 meV and that the softening is reduced even in the two mode hypothesis. These observations are thus consistent with a persisting anomaly at the stripe propagation wave-vector in a more metallic system, where both the doubling and the shift of the low energy mode appear to be reduced. Previous results obtained by IXS²⁶ on $\text{La}_{2-x}\text{Sr}_x\text{CuO}_{4+\delta}$ for different doping level are interpreted in the standard cosine-like dispersion picture, but corresponds to a set-up with only ≈ 6 meV resolution, about twice the present one. A review of this anomaly in other HTCS is reported in Ref. 10. Finally, we note here that a possible link has recently been suggested in single layer $\text{Bi}_2\text{Sr}_{1.6}\text{La}_{0.4}\text{Cu}_2\text{O}_{6+\delta}$ ²⁷ between the maximum of the Cu-O bond stretching softening and width, and a Fermi surface nesting vector at $q_x \approx 0.22$, with a clear kink in the electron dispersion at the energy of the phonon mode. The vector is close to the stripe propagation vector in double layer $\text{Bi}_{2-x}\text{Sr}_2\text{CaCu}_2\text{O}_{8+\delta}$ reported by STM in Ref. 28 and very recently in single layer $\text{Bi}_{2-y}\text{Pb}_y\text{Sr}_{2-z}\text{La}_z\text{Cu}_2\text{O}_{6+x}$ ²⁹. This correlation suggests that stripes are closer to the classical charge-density-wave, which in fact fully develops in others systems as bismuthates, with similar effects on the Bi-O bond stretching modes³⁰. In order to confirm this hypothesis, however, further investigations, similar to the one of Ref. 27, on others systems and dopings are required.

IV. CONCLUSIONS

We directly observe a sharp dip in the dispersion of the Cu-O bond-stretching or half-breathing mode at the wave-vector $q_x \sim 0.3$ associated with the stripe propagation-vector, as previously suggested in Ref. 10. Our data are consistent with the two mode hypothesis, which would describe this softening as associated with a doubling of the mode, possibly due to a splitting of the doubly degenerate Cu-O bond-stretching mode¹⁰. Our observation shows that the effect persists in a superconducting system close to optimal doping.

Acknowledgments

We acknowledge D. Gambetti for technical help. This work was supported by ESRF through experiment HS-3460. The IXS measurements and data analysis were partially supported by the Director, Office of Science, Office of Basic Energy Sciences, Materials Sciences and Engineering Division, of the U.S. Department of Energy under Contract No. DE-AC02-05CH11231. We acknowledge the support of the National Science Foundation through Grant No. DMR-0349361 and DMR-0405682, as well as of the University of California, Berkeley, through France Berkeley Fund Grant.

-
- ¹ L. Pintschovius and W. Reichardt, in *Physics and Chemistry of Materials with Low-Dimensional Structures*, edited by A. Furrer (Kluwer Academic Publishers, Dordrecht, 1998), vol. 20, p. 165.
- ² J. Zaanen and O. Gunnarsson, *Phys. Rev. B* **40**, 7391 (1989).
- ³ K. Machida, *Physica* **C158**, 192 (1989).
- ⁴ M. Kato, K. Machida, H. Nakanishi, and M. Fujita, *J. Phys. Soc. Jpn.* **59**, 1047 (1990).
- ⁵ S. A. Kivelson, E. Fradkin, and V. J. Emery, *Nature* **393**, 550 (1998).
- ⁶ S. A. Kivelson, I. P. Bindloss, E. Fradkin, V. Oganesyan, J. M. Tranquada, A. Kapitulnik, and C. Howald, *Rev. Mod. Phys.* **75**, 1201 (2003).
- ⁷ R. J. McQueeney, Y. Petrov, T. Egami, M. Yethiraj, G. Shirane, and Y. Endoh, *Phys. Rev. Lett.* **82**, 628 (1999).
- ⁸ L. Pintschovius and M. Braden, *Phys. Rev. B* **60**, R15039 (1999).
- ⁹ F. Giustino, M. L. Cohen, and S. G. Louie, *Nature* **452**, 975 (2008).
- ¹⁰ D. Reznik, L. Pintschovius, M. Ito, S. Iikubo, M. Sato, H. Goka, M. Fujita, K. Yamada, G. Gu, and J. Tranquada, *Nature* **440**, 1170 (2006).
- ¹¹ A. R. Moodenbaugh, Y. Xu, M. Suenaga, T. J. Folkerts, and R. N. Shelton, *Phys. Rev. B* **38**, 4596 (1988).
- ¹² M. Fujita, H. Goka, K. Yamada, J. M. Tranquada, and L. P. Regnault, *Phys. Rev. B* **70**, 104517 (2004).
- ¹³ P. Abbamonte, A. Ruydy, S. Smadici, G. Gu, G. Sawatzky, and D. Feng, *Nature Physics* **1**, 155 (2005).
- ¹⁴ Y.-J. Kim, G. D. Gu, T. Gog, and D. Casa, *Physical Review B (Condensed Matter and Materials Physics)* **77**, 064520 (2008).
- ¹⁵ M. Vojta, T. Vojta, and R. K. Kaul, *Physical Review Letters* **97**, 097001 (2006).
- ¹⁶ V. Hinkov, P. Bourges, S. Pailhs, Y. Sidis, A. Ivanov, C. D. Frost, T. G. Perring, C. T. Lin, D. P. Chen¹, and B. Keimer, *Nature Physics* **3**, 780 (2007).
- ¹⁷ J. Graf, M. d'Astuto, P. Giura, A. Shukla, N. L. Saini, A. Bossak, M. Krisch, S.-W. Cheong, T. Sasagawa, and A. Lanzara, *Phys. Rev. B* **76**, 172507 (2007).
- ¹⁸ J. D. Axe, A. H. Moudden, D. Hohlwein, D. E. Cox, K. M. Mohanty, A. R. Moodenbaugh, and Y. Xu, *Phys. Rev. Lett.* **62**, 2751 (1989).
- ¹⁹ C. Masciovecchio, U. Bergmann, M. Krisch, G. Ruocco, F. Sette, and R. Verbeni, *Nucl. Instrum. Meth. B* **111**, 181 (1996).
- ²⁰ M. Krisch and F. Sette, in *Light Scattering in Solids IX*, edited by M. Cardona and R. Merlin (Springer-Verlag Berlin, Heidelberg, 2007), vol. 108 of *Topics in Applied Physics*, p. 317.
- ²¹ R. Verbeni, F. Sette, M. Krisch, U. Bergmann, B. Gorges, C. Halcoussis, K. Martel, C. Masciovecchio, J. Ribois, G. Ruocco, et al., *J. Synchrotron Radiation* **3**, 62 (1996).
- ²² R. Verbeni, M. d'Astuto, M. Krisch, M. Lorenzen, A. Mermet, G. Monaco, H. Requardt, and F. Sette, *Rev. Sci. Instrum.* **79**, 083902 (2008).
- ²³ A. Mirone, *OpenPhonon code source* (2001), available on <http://www.esrf.fr/computing/scientific/>.
- ²⁴ S. L. Chaplot, W. Reichardt, L. Pintschovius, and N. Pyka, *Phys. Rev. B* **52**, 7230 (1995).
- ²⁵ J. M. Tranquada, K. Nakajima, M. Braden, L. Pintschovius, and R. J. McQueeney, *Phys. Rev. Lett.* **88**, 075505 (2002).
- ²⁶ T. Fukuda, J. Mizuki, K. Ikeuchi, K. Yamada, A. Q. R. Baron, and S. Tsutsui, *Physical Review B (Condensed Matter and Materials Physics)* **71**, 060501(R) (2005).
- ²⁷ J. Graf, M. d'Astuto, C. Jozwiak, D. R. Garcia, N. L. Saini, M. Krisch, K. Ikeuchi, A. Q. R. Baron, H. Eisaki, and A. Lanzara, *Physical Review Letters* **100**, 227002 (2008).
- ²⁸ J. E. Hoffman, E. W. Hudson, K. M. Lang, V. Madhavan, H. Eisaki, S. Uchida, and J. C. Davis, *Science* **295**, 466 (2002).
- ²⁹ W. D. Wise, M. C. Boyer, T. K. K. Chatterjee, T. Takeuchi, H. Ikuta, Y. Wang, and E. W. Hudson, *Nature Physics* **4**, 696 (2008).
- ³⁰ M. Braden, W. Reichardt, A. S. Ivanov, and A. Y. Rumiantsev, *Europhys. Lett.* **34**, 531 (1996).
- ³¹ G. Grüner, *Density Waves in Solids* (Addison-Wesley, Reading, MA, 1994).
- ³² The “classical” Kohn-anomaly is due to electron phonon coupling and in its strongest form can result in a charge density wave. The wave vector related to this effect is given by a nesting vector of the Fermi surface³¹. In the case of a stripe related anomaly, the difference is that stripes are supposed to originate from strong on-site coulomb repulsion⁵ and are not linked to the Fermi surface topology.